Mineralogical Magazine, August 2018, Vol. 82(4), pp. 961–973

Hydrothermal synthesis and characterization of kalsilite by using a kaolinitic rock from Sardinia, Italy, and its application in the production of biodiesel

Daniela Novembre[1,*], Domingo Gimeno[2], Nicola d'Alessandro[1] and Lucia Tonucci[3]

[1] Dipartimento di Ingegneria e Geologia, Università degli Studi "G. d'Annunzio", 66013 Chieti, Italy
[2] Dept. de Mineralogia, Petrologia i Geologia Aplicada, Universitat de Barcelona, 08028 Barcelona, Spain
[3] Dipartimento di Scienze Filosofiche, Pedagogiche ed Economico-Quantitative, Università degli Studi "G. d'Annunzio", 66013 Chieti, Italy

[*Received 9 March 2017; Accepted 16 October 2017; Associate Editor: Andrew Christy*]

ABSTRACT

The present work deals with the synthesis of kalsilite using material from a kaolinitic rock outcrop in Romana, Sassary Province, Sardinia, Italy.

The hydrothermal synthesis method required the dissolution of kaolin and $Al(OH)_3$ in a KOH solution at a temperature of 190°C and 1.013 bar. Crystallization of kalsilite was confirmed at 12 h in association with kaliophilite H2 as a metastable phase.

The products of synthesis were fully characterized by powder X-ray diffraction, scanning electron microscopy, inductively coupled plasma optical emission spectrometry, infrared spectroscopy and ^{29}Si nuclear magnetic resonance. The amorphous phase in the synthesis powders was estimated with quantitative phase analysis using the combined Rietveld and reference intensity ratio methods. Cell parameters and density were also calculated for the kalsilite. A potential application of kalsilite was investigated as a heterogeneous catalyst for biodiesel synthesis from sunflower oil used for frying.

Keywords: hydrothermal synthesis, kalsilite, biodiesel.

Introduction

The feldspathoid $KAlSiO_4$ has, like zeolites, a framework structure of linked $(Si, Al)O_4$ tetrahedra. The first structural refinement of kalsilite was performed by Perrotta and Smith (1965) who studied a natural sample of kalsilite from Mt. Nyiragongo, Congo, naming it "low kalsilite" (hexagonal symmetry, space group $P6_3$, $a = 5.161$ and $c = 8.699$ Å). Andou and Kawahara (1984) synthesized low kalsilite under hydrothermal conditions (600°C and 15 days), also with hexagonal symmetry ($a = 5.151$ and $c = 8.690$ Å); low kalsilite was later also synthesized by Okamoto (1997) (600°C and 14 days), with an observed modification at high temperature (above 865°C) into the high kalsilite polymorph ($P6_3mc$ or $P6_3/mmc$). Kawahara *et al.* (1987) investigated transformation of low kalsilite into high kalsilite at 865°C.

Several applications for kalsilite have been developed in the past, for example as an ingredient in dental ceramic materials (Kumar *et al.*, 2015). Kalsilite crystallization may be related to the formation mechanism of leucite; in fact, it was observed that when synthesizing leucite for biomedical applications, kalsilite crystallizes as a metastable intermediate reaction product and then disappears after prolonged heating (Zhang *et al.*, 2007). Also Bogdanoviciene *et al.* (2007) reported that during the preparation of alumosilicate glass ceramics the synthesis of multiphasic products (kalsilite, leucite and sanidine) very often occurs.

Recently, kalsilite was used as a heterogeneous catalyst for transesterification of soybean oil with

*E-mail: daniela.novembre@unich.it
https://doi.org/10.1180/minmag.2017.081.080

methanol to biodiesel (Wen *et al.*, 2010). At present, biodiesel is produced principally by the transesterification reaction of vegetable oils in the presence of methanol and homogeneous alkaline catalysts. The final product (fatty acid methyl ester) is purified by removing glycerol, various by-products present in minor amounts and a homogeneous catalyst (e.g. KOH). Although recycling of glycerol could make this process more efficient (Canale *et al.*, 2014), the classical biodiesel production procedure is still laborious, making it not fully sustainable economically. The use of a heterogeneous catalyst, such as kalsilite, could improve the entire process by reducing and making the purification more efficient. A few studies have reported the use of kalsilite as a transesterification catalyst in the presence of soybean oil and methanol at 120°C (weight ratio: oil/methanol/kalsilite = 100/50/5) (Wen *et al.*, 2010).

Kalsilite has been synthesized in the past by various techniques, including cation exchange from nepheline (Dollase and Freeborn, 1977); a sol-gel method using TEOS or SiO_2 (Hamilton and Henderson, 1968; Bogdanoviciene *et al.*, 2007); hydrothermal methods (Smith and Tuttle, 1957; Kopp *et al.*, 1961; Andou and Kawahara, 1984; Okamoto and Kawahara, 1996; Okamoto, 1997; Becerro *et al.*, 2009*a*,*b*); and solid-state synthesis from zeolite, silicate compounds and kaolinite (Dimitrijevic and Dondur, 1995; Heller-Kallai and Lapides, 2003; Kosanovic *et al.*, 1997).

With the aim of using kaolinite as a starting material, our research group conducted several studies on the reactivity of 'metakaolinite' (dehydroxylated kaolinite) with alkali solutions in successful zeolitic synthesis (Novembre *et al.*, 2005, 2010, 2011, 2014). However, few reports have been published on the direct kalsilite synthesis from kaolin, avoiding the use of any chemicals ('green conditions'). We can only cite the work of Becerro *et al.* (2009*a*) and Becerro *et al.* (2009*b*) who synthesized kalsilite by hydrothermal treatment of kaolin at 300°C for 12 h in a KOH solution.

The present work seeks to extract value from an abandoned kaolin quarry, as well as aiming towards realization of a 'green' mineralogical synthesis process. The scope of the present work is in fact to synthesize kalsilite by the hydrothermal technique using a kaolinitic rock from northern Sardinia, Italy, lowering the synthesis temperature as far as possible and obtaining a higher yield than reached in the past by other authors.

Furthermore, we tried to employ the synthesized kalsilite as a heterogeneous green catalyst in the production of biodiesel starting from a non-edible, cheap and largely available product such as sunflower oil that has been used for frying. The process is particularly sustainable as non-toxic and inexpensive catalysts are easily available. Furthermore, we should emphasize that this is an example of adding value to readily available by-products as reported in other studies for lignin-based derivatives that are another important class of agroindustrial waste (Tonucci *et al.*, 2012; Girardi *et al.*, 2014). Use of other cheap kaolin sources and blends of used non-edible oils could be envisaged in similar future experiments.

Experimental

Materials

The kaolin samples used as starting material in our work were collected from an outcrop at the Locchera quarry (Fig. 1), in Romana, Sassari province, Sardinia, Italy. Kaolin from the Locchera quarry is cryptocrystalline, shows a thickness of ~20 m and generally appears compact and slightly oily.

The kaolin was triturated, and the sandy fraction was separated by retention in a sieve. The fraction below 90 μm was then collected, suspended in distilled water, sonicated and centrifuged for separation of the silt fraction and collection of the clay fraction.

All the chemical reagents used in the synthesis protocol were purchased from Honeywell Riedel-de-Haën™ products (the purities of the reagents were ≥ 99%). The sunflower oil was a commercial product, purchased at a local supermarket; it was used to fry frozen chips for 10 min.

Synthesis of kalsilite

A solution of 0.86 M KOH was prepared by dissolving 1.35 g of KOH pellets in 28 mL of distilled water. Then 0.8 g of $Al(OH)_3$ (65%, p/v) and 3.10 g of kaolin were mixed with the KOH solution. The resulting mixture was put inside a stainless-steel hydrothermal reactor and heated at 10°C/min until 190°C and kept for 12, 15 and 18 h.

Kalsilite catalysed transesterification of sunflower oil

Both fresh oils and those used for frying were titrated with KOH 0.1 M to establish the % of free fatty acids, expressed as oleic acid,

https://doi.org/10.1180/minmag.2017.081.080 Published online by Cambridge University Press

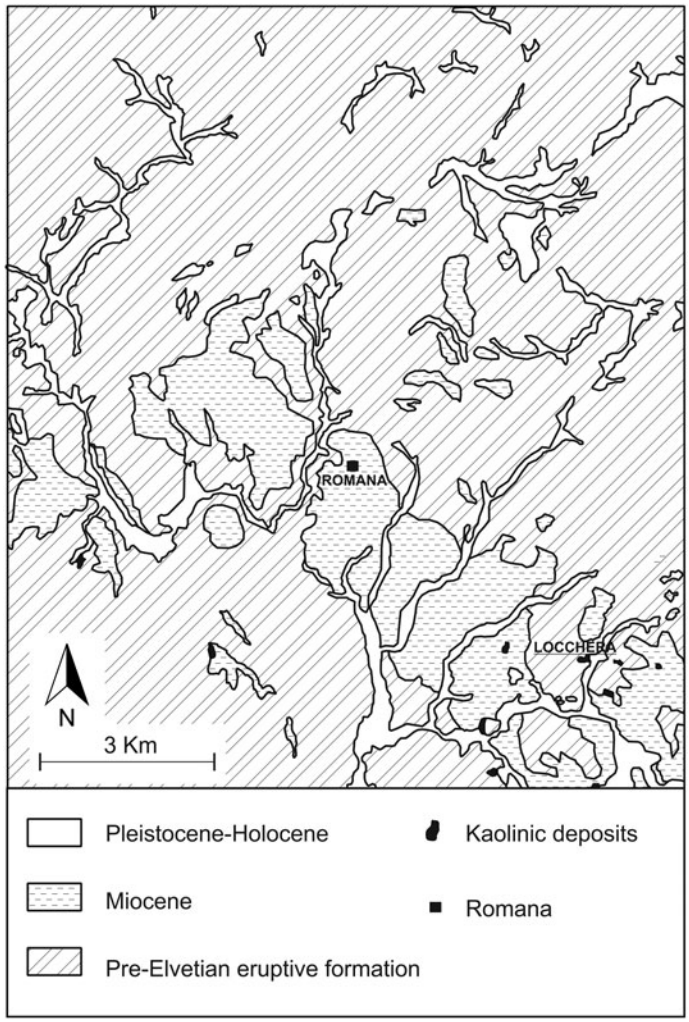

FIG. 1. Geological sketch map of the Romana area.

following the common methodology for edible vegetable oils (AOAC Official Method 940.28 free fatty acids in crude and refined oils). Kalsilite was tested as the transesterification catalyst; the commercial edible sunflower oil and the filtered used oil in the presence of methanol, at 50°C, were stirred for 5 h (weight ratio: oil/methanol/kalsilite = 100/20/0.75). The 'biodiesel phase' was separated by using a separating funnel and washed three times with NaCl saturated aqueous solution. It was then characterized by ^{1}H NMR (nuclear magnetic resonance) using $CDCl_3$ as the solvent.

Characterization methods

Romana kaolin and synthesized powders were analysed by powder X-ray diffraction (PXRD); the instrument was a Siemens D5000 operating with a Bragg-Brentano geometry using Cu$K\alpha$ radiation (λ=1.518 Å) at 40 kV and 40 mA, 4–45° scanning interval, step size 0.020°2θ with 10 s step^{-1}, a divergence slit of 0.5° and a receiving slit of 0.1 mm.

Synthetic samples, collected at different time intervals, were washed thoroughly with distilled water and oven dried at 40°C for 24 h.

https://doi.org/10.1180/minmag.2017.081.080 Published online by Cambridge University Press

TABLE 1. Chemical composition of Romana kaolin.

Oxides	Wt.%	Oxides	Wt.%
SiO_2	70.17	CaO	0.02
TiO_2	0.02	Na_2O	0.03
Al_2O_3	21.34	K_2O	0.04
Fe_2O_3	0.04	P_2O_5	0.02
MgO	trace	H_2O*	9.30

* Loss on ignition

Identification of mineral phases and relative peak assignments were performed with reference to the following JCPDS codes (powder diffraction files from the International Centre for Diffraction Data, http://www.icdd.com/): 00-011-0579 for kalsilite and 00-011-0313 for kaliophilite H2. Both the crystalline and amorphous phases in the synthesis powders were estimated using Quantitative Phase Analysis (QPA) applying the combined Rietveld and Reference Intensity Ratio (RIR) methods; corundum NIST 676a was added to each sample, amounting to 10% (according to the strategy proposed by Gualtieri, 2000 and Novembre *et al.*, 2017), and the powder mixtures were homogenized by hand-grinding in an agate mortar. Data for the QPA refinement were collected in the angular range 5–110°2θ with steps of 0.02°2θ and 10 s step^{-1}, a divergence slit of 0.5° and a receiving slit of 0.1 mm. Data were processed with the *GSAS* software (Larson and Von Dreele, 1997) and the graphical interface *EXPGUI* (Toby, 2001). The unit-cell parameters were determined, starting with the structural models proposed by Andou and Kawahara (1984) for kalsilite. The following parameters were refined: background parameters, zero shift, cell parameters and peak profiles.

Fourier-transform infrared analyses (FTIR) of Romana kaolin and the synthesized products were conducted with an ABB FTLA2000 spectrometer, equipped by a separator of KBr and a DTGS detector; the source of IR radiation was a SiC (Globar) filament. Samples were treated according to the method of Robert *et al.* (1989) using powder pressed pellets (KBr/sample ratio of 1/100, pressure undergone prior determination 15 t/cm^2); spectra were processed with the program *GRAMS-AI* (ThermoFisher scientific), spectral range: 650–3800 cm^{-1}.

Morphological analyses were carried out with a scanning electron microscope (SEM); the instrument was a JEOL JSM-840, with operating conditions of 15 kV and window ranging from 18 to 22 mm following the procedure reported in Ruggieri *et al.* (2010), and a double coating (gold and graphite) procedure.

Kaolin composition was determined by X-ray fluorescence (XRF), by means of a Sequential X-Ray Spectrophotometer PHILIPS PW 2400. Major-element determination was carried out using fused

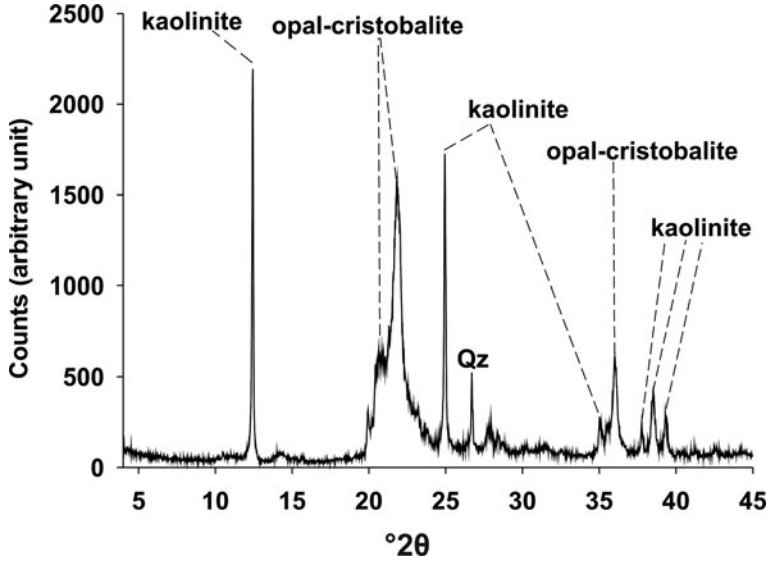

FIG. 2. Diffraction pattern of raw kaolin.

https://doi.org/10.1180/minmag.2017.081.080 Published online by Cambridge University Press

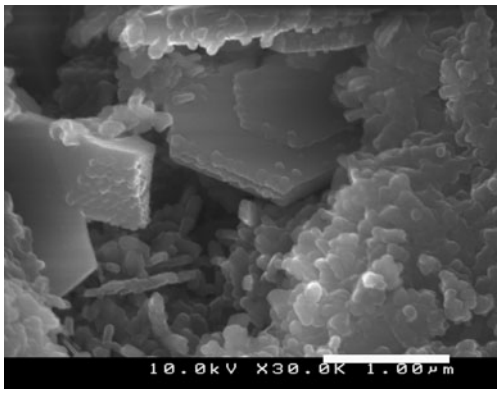

FIG. 3. Scanning electron microscope images of raw kaolin showing prismatic particles of kaolinite.

beads (lithium tetraborate pearls at a dilution 1/20). The beads were made in triplicate in Pt crucibles and collector dishes, using LiI as a viscosity corrector, and were determined two times (original and duplicate; the third bead was used to clean the crucible which was also cleaned regularly with nitric acid). All the samples were carefully treated at 130°C in pyrex receptacles for 48 h prior to any other manipulation. We also obtained a value for the loss on ignition of 1 g of sample using a ceramic crucible in an oxidizing furnace.

Chemical analysis of synthesized powders was carried out with inductively coupled plasma optical emission spectroscopy (ICP-OES, Perkin Elmer Optima 3200 RL) following the procedure reported in Fernandez-Turiel *et al.* (2003) preceded by fusion in lithium meta-tetraborate beads and subsequent acid solubilization.

The density of kalsilite was calculated by He-pycnometry using an AccuPyc 1330 pycnometer as explained in Novembre *et al.* (2004).

The NMR spectra were obtained using a Bruker Avance 300 spectrometer (7.05 Tesla) equipped with a high-resolution multinuclear probe that operated in the range of 30 MHz to 300 MHz and with a two-channel magic angle spinning (MAS) NMR probe using magic angle spinning speeds up to 5 kHz with standard Zirconia rotors with 7 mm of diameter. Spectra were processed by *XWINNMR* (Bruker program). Synthesized kalsilite was analysed using ^{29}Si MAS NMR (4000 Hz speed of rotation, 100–400 scans, 8 µs 90° excitation pulse and 5 s relaxation delay time). The chemical shifts were referenced to trimethylsilyl propionic (2,2,3,3)- d_4 acid, sodium salt (TSP) for ^{29}Si. The ^{1}H NMR spectra in $CDCl_3$ solution were acquired in a NMR tube (5 mm) using tetramethylsilane as reference. A standard pulse sequence (zg) with a spectral width of –0.5 ppm to 12.5 ppm, a 90° excitation pulse (7.6 µs) and 1 s relaxation delay time was used to collect 32 scans.

Results and discussion

Characterization of the starting material

The chemical composition of kaolin is reported in Table 1. Romana kaolin shows a silica excess with

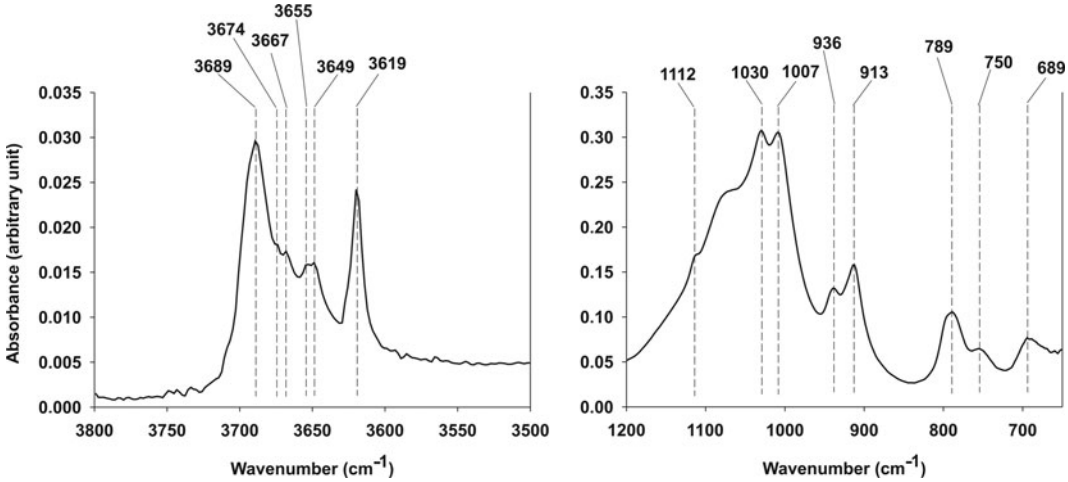

FIG. 4. FTIR spectra of starting material. Left: high frequency range (3800–3500 cm^{-1}); right: low frequency range (1200–650 cm^{-1}).

https://doi.org/10.1180/minmag.2017.081.080 Published online by Cambridge University Press

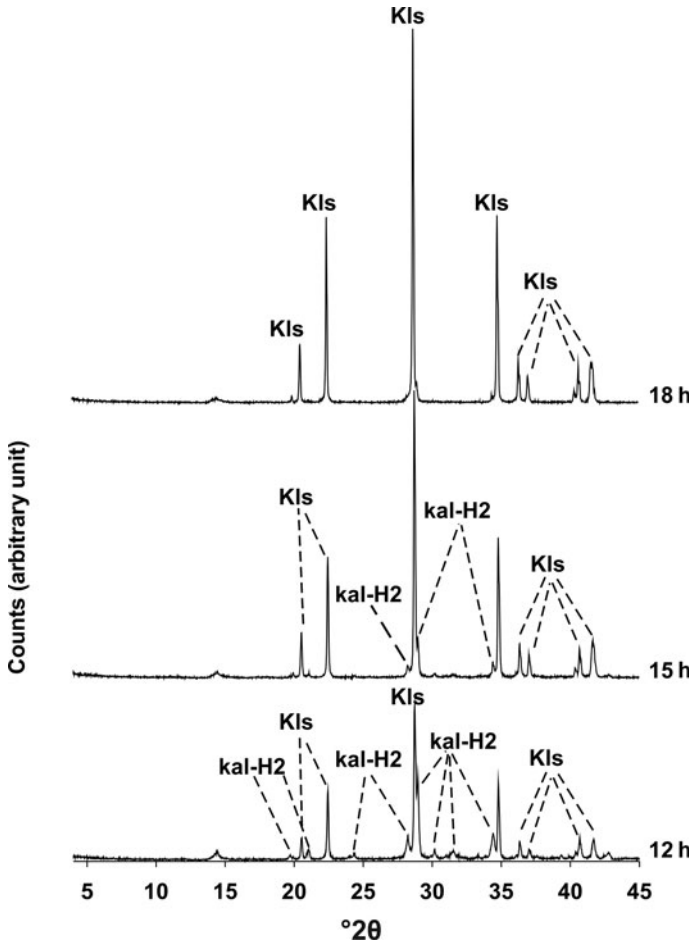

FIG. 5. X-ray diffractometric sequence of the synthesis run. Kal-H2: Kaliophilite H2; Kls: kalsilite.

respect to pure kaolinite, and the PXRD data were consistent with this observation, revealing a mineral assemblage of kaolinite plus small amounts opal/cristobalite and quartz (Fig. 2). This peculiar characteristic gives the material a Si/Al ratio greater than 1, unlike the typical commercial kaolins. For this characteristic and if $Al(OH)_3$ was not added, Romana kaolin would be a material suitable for synthesis of minerals characterized by Si/Al ratio greater than 1, such as leucite type, silica-rich zeolites, etc. For the present study, with the intent of synthesizing kalsilite, $Al(OH)_3$ was added to bring the kaolin stoichiometry to a Si/Al ratio of 1.

The morphological analysis showed that kaolin particles had an irregular flake shape, with a micrometre-scale grain size (Fig. 3).

Infrared analysis was conducted on kaolin raw material (Fig. 4). The bands between 3750 and 3500 cm^{-1} are attributed to –OH stretching. In particular five bands were evidenced at 3649, 3655, 3667, 3674 and 3689 cm^{-1} and related to the inner surface –OH in-phase/out-of-phase stretching vibrations (Cheng *et al.*, 2010*a*; Frost *et al.*, 2001*b*); a band centred at 3619 cm^{-1} is related to the inner OH-stretching vibration. In the lower frequency region of the IR spectra (1800–400 cm^{-1}) a band at 1112 cm^{-1} was observed and attributed to the apical Si–O stretching vibration (Cheng *et al.*, 2010*b*); in the same frequency region two bands located, respectively, at 1030 and 1007 cm^{-1} were attributed to apical Si–O stretching vibrations (Cheng *et al.*, 2010*b*); two other bands at 936 and

https://doi.org/10.1180/minmag.2017.081.080 Published online by Cambridge University Press

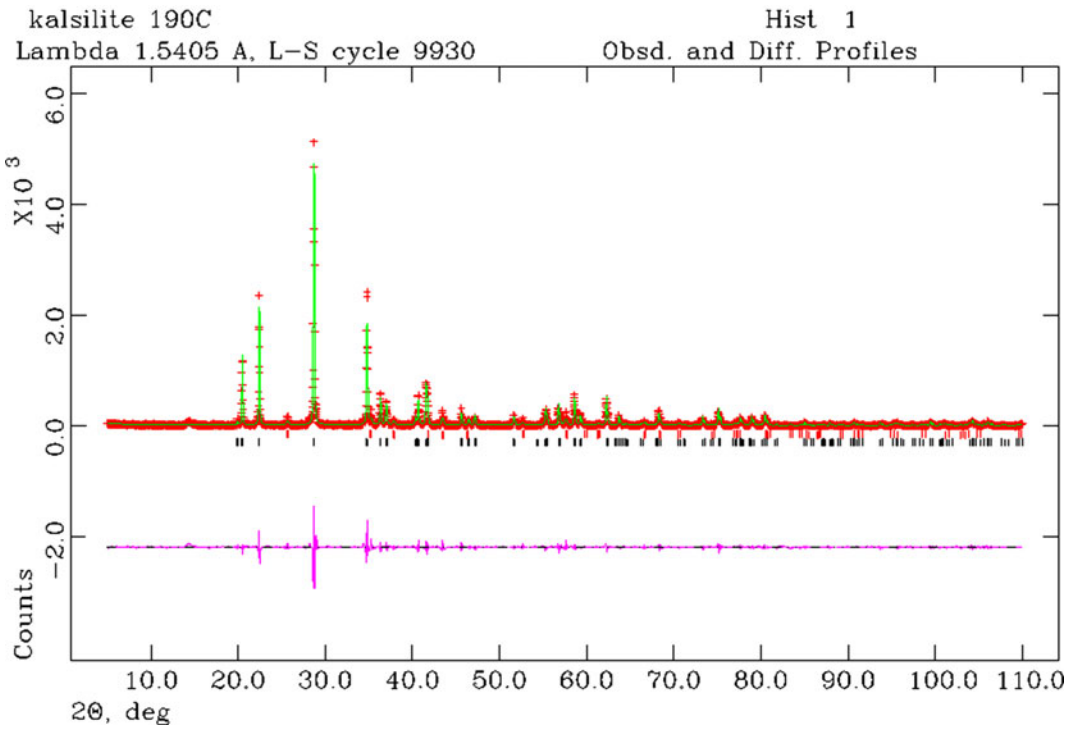

FIG. 6. Rietveld refinement plots: observed (red) and calculated profiles (green) and difference plot (pink) for kalsilite and corundum NIST 676a with tick marks at the positions of the Bragg peaks. Markers: kalsilite (black), corundum NIST 676a (red).

913 cm^{-1} were attributed to Al–OH bending vibrations (Qtaitat and Al-Trawneh, 2005); three bands at 789, 750 and 689 cm^{-1} were related to –OH (Al–OH) translational vibrations (Frost *et al.*, 2001*a*). A strong stretching band is located at 1050 cm^{-1} and related to the presence of opal–cristobalite.

Characterization of synthesized kalsilite

The crystallization of synthetic kaliophilite H2 as a metastable phase (*sensu* Tuttle and Smith, 1958) was verified by the PXRD analyses (Fig. 5) in the time interval 12–15 h along with kalsilite. The disappearance of kaliophilite was observed after 18 h, at which time kalsilite remained as a unique phase.

Rietveld refinement was performed on the products of reaction after 18 h. The observed and calculated profiles and difference plot for kalsilite and corundum NIST 676a with tick marks at the positions of the Bragg peaks are reported in Fig. 6. The cell parameters for kalsilite (Table 2), refined with a hexagonal symmetry, space group $P6_3$, were $a_0 = b_0 = 5.1652(57)$ Å and the $c_0 = 8.6894(49)$ Å. These parameters are in good agreement with those of Andou and Kawahara (1984).

The results of the QPA indicated that the calculated amorphous phase in the sample is 5.7(8)%, thus resulting in a final product of 94.3(8)% kalsilite.

The chemical formula of kalsilite, calculated by the chemical analyses reported in Table 3, is $K_{7.94}Al_{7.88}Si_{8.10}O_{32}$.

Morphological observations provided evidence of the crystalline growth of kalsilite hexagonal crystals of ~3 μm long (Fig. 7). Calculations gave a density of 2.609 g/cm^3, close to the value of 2.64 g/cm^3 reported in literature (Okamoto, 1997).

The FTIR spectrum for kalsilite revealed that tetrahedra present an asymmetric stretch of inner bonds at 963 cm^{-1} and a symmetric stretch of external bonds at 683 cm^{-1} (Fig. 8). For a

https://doi.org/10.1180/minmag.2017.081.080 Published online by Cambridge University Press

TABLE 2. Experimental conditions and crystallographic data for kalsilite plus 10% corundum NIST 676a: samples at 18 h into synthesis run.

Sample	18 h + 10% Corundum NIST 676a
Wavelength (Å)	1.5405
No. of observations	9930
R_{wp}	0.19
R_p	0.14
χ^2	2.54
% amorphous	5.7(8)
% kalsilite phase	94.3(8)
Space group kalsilite	$P6_3$
a (Å)	5.1652 (57)
b (Å)	5.1652 (57)
c (Å)	8.6894 (49)

comparison see Becerro *et al.* (2009*a*) and Henderson and Taylor (1988).

The ^{29}Si MAS-NMR spectrum of the products of hydrothermal treatment after 18 h of reaction time (Fig. 9) revealed a single unique peak located at –88.7 ppm. Data are consistent with those reported for this mineral (Becerro *et al.*, 2009*a*; Dimitrijevic and Dondur, 1995).

To evaluate the acid/base character of kalsilite, we performed some tests with several pH indicators. The basic character was clearly evident as a pink colour appeared on suspending kalsilite in a phenolphthalein methanol solution (pKa = 9.7). However, when we carried out the same experiment with other pH indicators having higher pKa values (i.e. 4-chloro-2-nitroaniline; pKa = 17.2), we observed that the colour solution remained yellow, showing a basicity lower than our indicator.

TABLE 3. Chemical characterization (ICP-OES) of kalsilite. Values for the oxides, namely MgO, MnO, TiO_2 and P_2O_5, are below the detection limits.

Temperature (°C)	K_2O (%)	SiO_2 (%)	Al_2O_3 (%)	Time (h)	XRD spectrum
190	29.6	38.5	31.8	18	Kalsilite (strong)
(*)	28.5	39.3	31.6		

(*): Stebbins *et al.* (1986).

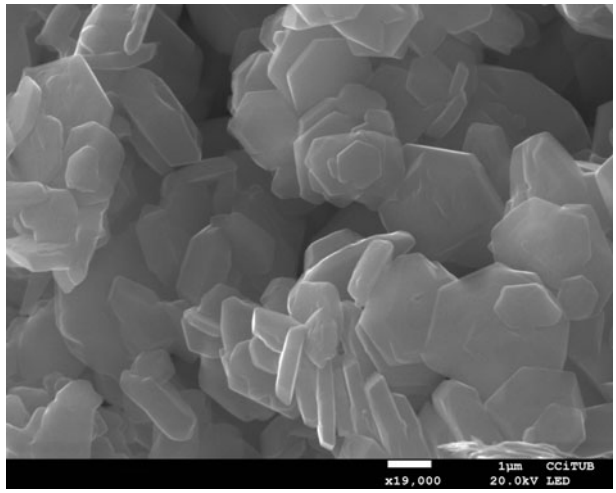

FIG. 7. Scanning electron microscope images of kalsilite at 18 h.

https://doi.org/10.1180/minmag.2017.081.080 Published online by Cambridge University Press

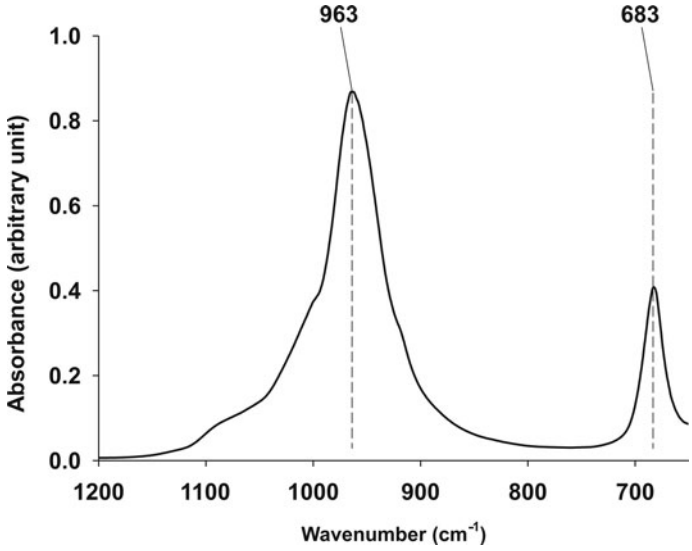

FIG. 8. Infrared spectrum of synthesized kalsilite.

Kalsilite as a potential catalyst for biodiesel synthesis

We tested kalsilite as a transesterification catalyst for sunflower oil, both fresh and used for frying, in presence of methanol at 50°C under vigorous stirring for 5 h. The oils were previously titrated to determine the free acidity that is crucial for the transesterification behaviour. It is known that oils with free acidity higher than 0.5% are not suitable for treatments with solid basic catalysts (Berrios *et al.*, 2010). The sunflower oil samples showed free acidity of 0.3% for the used oil, while no free acidity was detectable in the fresh oil. The starting oil gave a ^{1}H NMR spectrum typical for a triglyceride (Fig. 10*a*), where we can see all the characteristic signals: the methyl groups (at 1.0 ppm), the methylene fatty acid groups (from 1.3 to 3 ppm), the glyceride CH_2 (from 4.2 to 4.5 ppm) and the unsaturated hydrogens plus the glyceride 2-CH (superimposed; at 5.3–5.6 ppm). At the beginning of the transesterification reaction, after the addition of methanol, we also observed, together with the previous signals, the typical singlet of the alcoholic methyl group at 3.6 ppm (Fig. 10*b*). The experimental evidence that proves the efficiency of the transesterification step is the presence of the singlet at 3.8 ppm attributable to the methyl ester groups (Fig. 10*c*). In fact, this peak was detected in the reaction samples previously submitted to an extended evaporation step (removing all the free methanol). Even though methyl alcohol and methyl esters possess similarly shaped signals, the shift of 0.2 ppm (from 3.6 to 3.8 ppm) demonstrates the presence of methyl esters. Transesterification yields were calculated by comparing the area of the signal relative to the methyl groups (1 ppm) with the area of the signal relative to the methyl ester group.

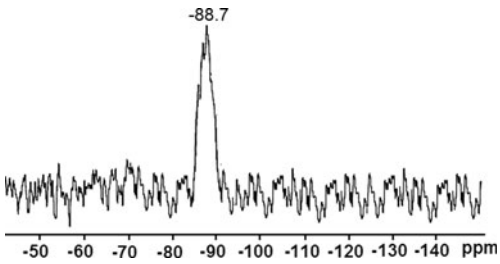

FIG. 9. ^{29}Si MAS-NMR spectrum of synthesized kalsilite.

This result confirmed the activity of kalsilite as the transesterification catalyst even at a low concentration and mild temperature: we obtained, with the used oil, a triglyceride transformation yield of 20% using a catalyst-to-oil weight ratio of 1% at 50°C (25% yield with the edible, not used, oil). We note that Wen *et al.*, operating with a suitably modified kalsilite (with Li), obtained a total conversion but employed a 5% ratio of catalyst at a relatively higher temperature of 120°C.

Moreover, the use of an inedible but cheap and readily available oil such as used sunflower oil

https://doi.org/10.1180/minmag.2017.081.080 Published online by Cambridge University Press

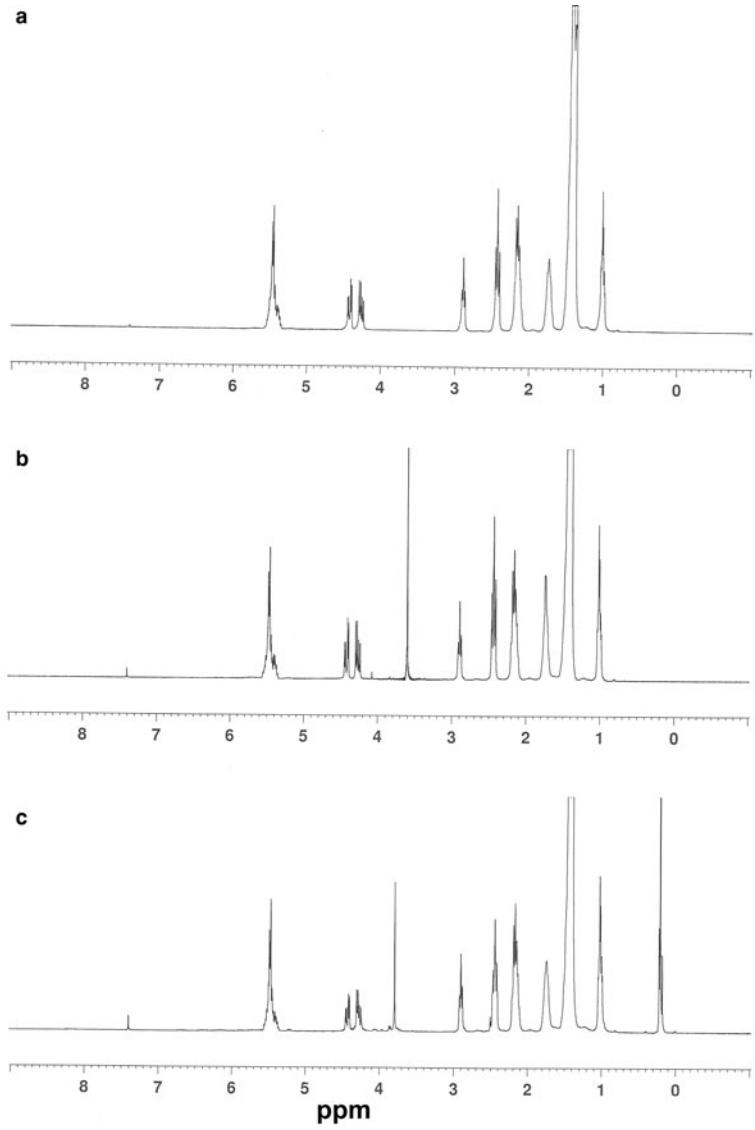

FIG. 10. ^{1}H NMR spectra in $CDCl_3$ of reaction mixture from used sunflower oil in presence of kalsilite as catalyst: (*a*) used oil alone; (*b*) reaction mixture at $t = 0$ min; and (*c*) final reaction mixture after vacuum evaporation (removing methanol).

allows for an environmentally friendly and low-cost synthetic process. In fact, the cost of refined vegetable oils contributed to nearly 80% of the overall biodiesel production cost (Lam *et al.*, 2009); thus the alternative use of waste cooking oil as feedstock to biodiesel can reduce the overall costs of biodiesel by more than half (Lam *et al.*, 2010).

Leung *et al.* (2010) reported that actually more than 95% of biodiesel has been obtained from edible oils. This can produce several ethical and economical concerns, as these edible oils (or the equivalent raw vegetables) are subtracted from human and animal food markets, leading to higher food prices. As an alternative, it would be simple to implement recovery of used cooking oils in public

https://doi.org/10.1180/minmag.2017.081.080 Published online by Cambridge University Press

eateries. We expect that used sunflower oil could become the dominant feedstock for biodiesel production in Europe, USA and much of the developed world, which vindicates our choice of this waste product for study.

Discussion and conclusions

This paper reports the synthesis and characterization of kalsilite from a kaolinitic rock, and its use in the production of biodiesel. The work both extracts further value from an abandoned kaolin quarry, and demonstrates a 'green' mineral synthetic process. Hydrothermal synthesis was at 190°C with pressure corresponding to the vapour pressure of water at that temperature. Crystallization of kalsilite was confirmed at 12 h in association with kaliophilite H2 as a metastable phase. After 18 h, kalsilite remained as the only silicate phase.

When comparing our work to those of other authors, a lowering of the costs of reagents, and an improvement in the temperature, yield and characterization of the final product is achieved. The temperature necessary for the transformation of kaolinite into kalsilite has been decreased from 300°C (Becerro *et al.*, 2009*a*,*b*) to 190°C, and although the reaction time had to be increased from 12 h to 18 h, an economization of the process was definitely achieved.

Becerro *et al.* (2009*a*,*b*), carried out the synthesis of kalsilite from a commercial kaolin that, as a starting material, is much more expensive than quarry recovery material. Generally, pure kaolin has a price ~$115/kg. More importantly, their yield was 70% and the final product contained a small percentage of anatase. In our case, however, a yield of 94.3% was achieved by quantitative analysis carried out using the QPA plus RIR methods.

The presence of opal/cristobalite in the kaolin does not represent an obstacle to the synthesis of kalsilite. As a matter of fact, Romana kaolin is used as a source of silica. The amorphous nature of some of the silica is advantageous from the point of view of reaction thermodynamics and kinetics. Similar benefits in reaction time and cost are widely documented in the literature referring to the synthesis of minerals (Novembre *et al.*, 2004, 2011, 2014; Chaisena and Rangsriwatananon, 2005).

This work has shown firstly that natural, impure kaolin can be used for environmentally friendly kalsilite synthesis at moderate temperature and hence low cost. Secondly, we have demonstrated that kalsilite can be used as an active transesterification catalyst with advantages in terms of low catalyst-to-oil value and low working temperature. The entire procedure, from the kalsilite synthesis to the transesterification step, can be considered particularly 'green and low-cost'. The fact that the catalysed reaction also works with an inedible sunflower oil that has been used for frying, shows that kalsilite is a robust catalyst, able to be active even in the presence of several by-products formed during the cooking process.

Acknowledgements

The authors greatly acknowledge the technical staff at CCiT (UB) for their help during the development of the work. N.d'A. is grateful to the "Consorzio di Ricerca per l'Innovazione Tecnologica, la Qualità e la Sicurezza degli Alimenti S.C.R.L." (ITQSA) (CIPE fundings 20.12.04; DM 28497) for financial support.

References

Andou, Y. and Kawahara, A. (1984) The refinement of the structure of synthetic kalsilite. *Mineralogical Journal*, **12**, 153–161.

Becerro, A.I., Escudero, A. and Mantovani, M. (2009*a*) The hydrothermal conversion of kaolinite to kalsilite: Influence of time, temperature, and pH. *American Mineralogist*, **94**, 1672–1678.

Becerro, A.I., Mantovani, M. and Escudero, A. (2009*b*) Hydrothermal synthesis of kalsilite: a simple and economical method. *Journal of the American Ceramic Society*, **92**, 2204–2206.

Berrios, M., Martín, M.A., Chica, A.F. and Martín, A. (2010) Study of esterification and transesterification in biodiesel production from used frying oils in a closed system. *Chemical Engineering Journal*, **160**, 473–479.

Bogdanoviciene, I., Jankeviciute, A., Pinkas, J., Beganskiene, A. and Kareiva, A. (2007) Sol-gel synthesis and characterization of Kalsilite-type alumosilicates. *Materials Science-Medziagotyra*, **13**, 3, 1392–1320.

Canale, V., Tonucci, L., Bressan, M. and d'Alessandro, N. (2014) Deoxydehydration of glycerol to allyl alcohol catalyzed by rhenium derivatives. *Catalysis Science and Technology*, **4**, 3697–3704.

Chaisena, A. and Rangsriwatananon, K. (2005) Synthesis of sodium zeolites from natural and modified diatomite. *Materials Letters*, **59**, 1474–1479.

Cheng, H., Liu, Q., Zhang, J., Yang, J. and Frost, R.L. (2010*a*) Delamination of kaolinite-potassium acetate intercalates by ball-milling. *Journal of Colloid and Interface Science*, **348**, 355–359.

https://doi.org/10.1180/minmag.2017.081.080 Published online by Cambridge University Press

Cheng, H., Yang, J., Liu, Q., Zhang, J. and Frost, R.L. (2010*b*) A spectroscopic comparison of selected Chinese kaolinite, coal bearing kaolinite and halloysite – A mid-infrared and near-infrared study. *Spectrochimica Acta A*, **77**, 856–861.

Dimitrijevic, R. and Dondur, V. (1995) Synthesis and characterization of $KAlSiO_4$ Polymorphs on the SiO_2–$KAlO_2$ join. II. The end-member of ANA-type zeolite framework. *Journal of the Solid State Chemistry*, **115**, 214–224.

Dollase, W.A. and Freeborn, W.P. (1977) The structure of $KAlSiO_4$ with $P6_3mc$ symmetry. *American Mineralogist*, **62**, 336–340.

Fernandez-Turiel, J.L., Gimeno, D., Rodríguez, J.J., Carnicero, M. and Valero, F. (2003) Factors influencing the quality of a surface water supply system: the Ter river, northeastern Spain. *Fresenius Environmental Bulletin*, **12**, 67–75.

Frost, R.L., Locos, O.B., Kristof, J.J. and Kloprogge, J.T. (2001*a*) Infrared Spectroscopic study of potassium and cesium acetate-intercalated kaolinites. *Vibrational Spectroscopy*, **26**, 33–42.

Frost, R.L., Makó, É., Kristóf, J., Horváth, É. and Kloprogge, J.T. (2001*b*) Modification of kaolinite surfaces by mechanochemical treatment. *Langmuir*, **17**, 4731–4738.

Girardi, F., Cichelli, A., Perri, E., Basti, C. and d'Alessandro, N. (2014) Oxidative treatments of solid olive residues: Effects on phenolic and fatty acid fractions. *European Journal of Lipid Science and Technology*, **116**, 352–359.

Gualtieri, A.F. (2000) Synthesis of sodium zeolites from a natural halloysite. *Physics and Chemistry of Minerals*, **28**, 719–728.

Hamilton, D.L. and Henderson, C.M.B. (1968) The preparation of silicate compositions by a gelling method. *Mineralogical Magazine*, **36**, 832–838.

Heller-Kallai, L. and Lapides, I. (2003) Thermal reactions of kaolinite with potassium carbonate. *Journal of Thermal Analysis and Calorimetry*, **71**, 689–698.

Henderson, C.M.B. and Taylor, D. (1988) The structural behaviour of the nepheline family: (3) Thermal expansion of kalsilite. *Mineralogical Magazine*, **52**, 708–711.

Kawahara, A., Andou, Y., Marumo, F. and Okomo, M. (1987) The crystal structure of high temperature form of kalsilite ($KAlSiO_4$) at 950°C. *Mineralogical Journal*, **13**, 260–270.

Kopp, O.C., Harris, L.A. and Clark, G.W. (1961) The hydrothermal conversion of muscovite to kalsilite and an iron-rich mica. *American Mineralogist*, **46**, 719–727.

Kosanović, C., Subotic, B., Šmit, I., Čižmek, A., Stubicar, M. and Tonejc, A. (1997) Study of structural transformations in potassium-exchanged zeolite A induced by thermal and mechanochemical treatments. *Journal of Material Science*, **32**, 73–78.

Kumar, P.H., Kumar Singh, V. and Kumar, P. (2015) Mechanochemically synthesized kalsilite based bioactive glass-ceramic composite for dental vaneering. *Applied Nanoscience*, 1–6.

Lam, M.K., Tan, K.T., Lee, K.T. and Mohamed, A.R. (2009) Malaysian palm oil: surviving the food versus fuel dispute for a sustainable future. *Renewable and Sustainable Energy Reviews*, **13**, 1456–1464.

Lam, M.K., Lee, K.T. and Mohamed, A.R. (2010) Homogeneous, heterogeneous and enzymatic catalysis for transesterification of high free fatty acid oil (waste cooking oil) to biodiesel: A review. *Biotechnology Advances*, **28**, 500–518.

Larson, A.C. and Von Dreele, R.B. (1997) General Structure Analysis System (GSAS). *Los Alamos National Laboratory Report Laur*, 86–748.

Leung, D.Y.C., Wu, X. and Leung, M.K.H. (2010) A review on biodiesel production using catalyzed transesterification. *Applied Energy Journal*, **87**, 1083–1095.

Novembre, D., Di Sabatino, B., Gimeno, D., Garcia Valles, M. and Martinez Manent, S. (2004) Synthesis of Na-X zeolites from tripolaceous deposits (Crotone, Italy) and volcanic zeolitised rocks (Vico Volcano, Italy). *Microporous and Mesoporous Materials*, **75**, 1–11.

Novembre, D., Di Sabatino, B. and Gimeno, D. (2005) Synthesis of Na-A zeolite from 10 Å halloysite and a new crystallization kinetic model for the transformation of Na-A into HS zeolite. *Clays and Clay Minerals*, **53**, 28–36.

Novembre, D., Gimeno, D., Pasculli, A. and Di Sabatino, B. (2010) Synthesis and characterization of sodalite using natural kaolinite: an analytical and mathematical approach to simulate the loss in weight of chlorine during the synthesis process. *Fresenius Environmental Bullettin*, **19**, 1109–1117.

Novembre, D., Di Sabatino, B., Gimeno, D. and Pace, C. (2011) Synthesis and characterization of Na-X, Na-A, and Na-P zeolites and hydroxysodalite from metakaolinite. *Clay Minerals*, **46**, 339–354.

Novembre, D., Pace, C. and Gimeno, D. (2014) Syntheses and characterization of zeolites K-F and W type using a diatomite precursor. *Mineralogical Magazine*, **78**, 1209–1225.

Novembre, D., Pace, C. and Gimeno, D. (2017) Synthesis and characterization of wollasonite 2M by using a diatomite precursor. *Mineralogical Magazine*, **82**, 95–110.

Okamoto, Y. (1997) Structural modification of $KAlSiO_4$ minerals. *Okayama University Earth Science Reports*, **4**, 41–72.

Okamoto, Y. and Kawahara, A. (1996) Interpretation of the crystal structure of synthetic kaliophilite from the domain structure of kalsilite. *Okayama University Earth Science Reports*, **3**, 57–64.

https://doi.org/10.1180/minmag.2017.081.080 Published online by Cambridge University Press

Perrotta, A.J. and Smith, J.V. (1965) The crystal structure of kalsilite, $KAlSiO_4$. *Mineralogical Magazine*, **35**, 588–595.

Qtaitat, M.A. and Al-Trawneh, I.N. (2005) Characterization of kaolinite of the Baten El-Ghoul region/south Jordan by infrared spectroscopy. *Spectrochimica Acta A*, **61**, 1519–1523.

Robert, J.L., Della Ventura, G. and Thauvin, J.L. (1989) The infrared OH-stretching region of synthetic richterites in the system Na_2O–K_2O–CaO–MgO–SiO_2–H_2O–HF. *European Journal of Mineralogy*, **1**, 203–211.

Ruggieri, F., Saavedra, J., Fernandez-Turiel, J.L., Gimeno, D. and Garcia-Valles, M. (2010) Environmental geochemistry of ancient volcanic ashes. *Journal of Hazardous Materials*, **183**, 353–365.

Smith, J.V. and Tuttle, O.F. (1957) The nepheline-kalsilite system; Part I, X-ray data for the crystalline phases. *American Journal of Science*, **255**, 282–305.

Stebbins, J.F., Murdoch, J.B., Carmichael, I.S.E. and Pines, A. (1986) Defects and short-range order in nepheline group minerals: a Silicon-29 Nuclear Magnetic Resonance study. *Physics and Chemistry of Minerals*, **13**, 371–381.

Toby, B.H. (2001) EXPGUI, a graphical user interface for GSAS. *Journal of Applied Crystallography*, **34**, 210–213.

Tonucci, L., Coccia, F., Bressan, M. and d'Alessandro, N. (2012) Mild photocatalysed and catalysed green oxidation of lignin: A useful pathway to low-molecular-weight derivatives. *Waste and Biomass Valorization*, **3**, 165–174.

Tuttle, O.F. and Smith, J.V. (1958) The nephelinekalsilite system; II, Phase relations. *American Journal Science*, **256**, 571–589.

Wen, G., Yan, Z., Smith, M., Zhang, P. and Wen, B. (2010) Kalsilite based heterogeneos catalyst for biodiesel production. *Fuel*, **89**, 2163–2165.

Zhang, Y., Lv, M., Chen, D. and Wu, J. (2007) Leucite cristallization kinetics with kalsilite as a transition phase. *Materials Letters*, **61**, 2978–2981.

https://doi.org/10.1180/minmag.2017.081.080 Published online by Cambridge University Press